

# Mutual positioning of automatically assembled noncylindrical parts

B. Bakšys\*, T. Sokolova\*\*

\*Kaunas University of Technology, Kęstučio 27, Kaunas, 44312 Lithuania, E-mail: Bronius.Baksys@ktu.lt

\*\*Kaunas University of Technology, Kęstučio 27, Kaunas, 44312 Lithuania, E-mail: Tatjana.Sokolova@ktu.lt

## 1. Introduction

Assembly is the final stage of the production, when the parts are arranged in respect of the each other according to the predetermined order [1]. One of the major problems in robotic automated assembly is the execution of tasks that require accurate relative positioning of the parts being assembled [2]. The process of automated assembly involves two main stages: mutual positioning of the connective surfaces and joining of the parts. The most important assembly problem is orientation and positioning of the connecting parts and directional matching of their surfaces before assembly. The conservative approach to this problem, to reduce misalignments using accurate handling equipment and parts, is becoming the less acceptable. The alternative is to apply accommodation techniques where contact forces between the parts modify their relative position or motion [2]. A compliance device combining passive and active compliance has been tested and developed for an anthropomorphic robot for the use during assembly operations. The device has the ability to correct angular and lateral misalignments between mating parts, resulting part damage. The method of control, the design features of the device and the modifications made to enable the device to be used for an anthropomorphic robot are described and future modifications which will the device enable to operate more effectively are discussed [3].

During the automated assembly noncylindrical connecting surfaces of the parts must take such a position, which makes it possible to join them using not only vibratory displacement but the turn of the parts. As were during positioning, the parts are located with respect of each other conforming predefined accuracy so, that it is possible to perform automated assembly [4].

Dry friction force arising between the part performing displacement and turn react against the matching of connecting surfaces of the parts. Friction is a natural phenomenon that occurs in many engineering systems. Technological possibilities of vibratory assembly may be expanded controlling the dry friction force, which arises between the surfaces of a moving body and a basing plane [4, 5].

In article [6] a new method of vibrotransportation on a plane surface moving in a circular law with dry friction control was suggested. Main features of the body motion on a plane were determined.

Dynamic investigation of vibrational transportation with dry controlled friction was presented in [7] work. Body vibrational transportation on a horizontal platform moving in harmonic law with dry controlled friction was created. It gives wide possibilities to control the body transportation parameters (velocity, direction) while changing platform horizontal harmonic vibrations amplitude and frequency and also the duration and control mo-

ments of effective dry friction between the transportation body and the platform with respect of vibration period. This way allows to fulfill special body transportation regimes such as disc shape body transportation by plane motion, i.e. give (impart) it transportational and rotational movements at the same time and to transport bodies in the necessary direction and trajectory on a circularly moving platform. Distribution of velocities and accelerations, also forces and their moments between disc-shaped body and platform are determined. The numerical investigation of every possible vibrotransportation regime defined by the dry friction effective factor control was performed. The longitudinal and rotatory motion interdependence of the disc - shaped body was defined on the basis of the experiment. Experimental investigations were fulfilled showing the alteration of the body motion direction while changing the high frequency vibrations of moment excitation with respect to the period of the platform moving in a circularly law and the possibilities of the body velocity control where indicated.

The results of mentioned analysis provide approximate information on vibrations influence on the dry friction coefficients, when it is necessary to perform appropriate positioning of the part with respect of the other part. The method of vibrotransportation under controlled dry friction may be successfully applied for automated mechanical assembly, manipulation and orientation of the parts and in other systems.

The main goal of this article is to analyze the vibratory displacement and turn of the body under dry friction force applying for automated assembly of the noncylindrical parts. By means of high frequency vibrations dry friction force of the body arising between contacting surfaces can be controlled changing the dry friction coefficients.

## 2. Dynamic model and differential equations of body

New assembly method, based on vibrational alignment of a movable body with respect to fixed body and controlling dry friction force are proposed in this article. During alignment the linear displacement and limited rotation of movable part take place.

Dynamic model of vibratory displacement and turn of the movable based body controlling dry friction is presented in Fig. 1. In order the moving body could perform the turn, a force moment should be created. Bushing of mass  $m$  (body 3 is fixed in jig 2) is based on two-part platform 1. Each part of the platform is excited by autonomous high frequency (piezoceramic) vibrators, causing elastic vibrations of the mentioned parts. Elastic ( $c_{x1}$ ,  $c_{x2}$ ) and damping ( $h_{x1}$ ,  $h_{x2}$ ) elements prevent displacement of the body while angular elasticity ( $c_{\varphi}$ ) pre-

vents the turn of the body. By means of elastic elements  $c_{y1}$  and  $c_{y2}$  the body may be pressed by the fixed force to the platform, which is excited by low frequency harmonic ( $A \sin \omega t$ ) vibrations in the predetermined direction at angle  $\beta$ .

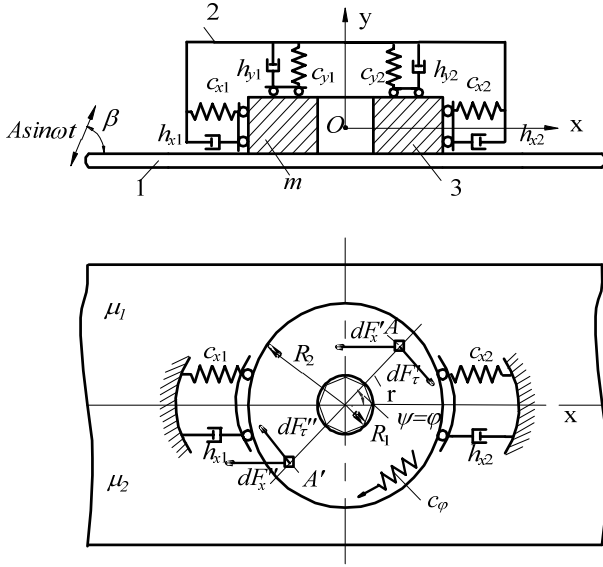


Fig. 1 Dynamical model of vibratory displacement and the turn of movably based body in assembly device

The motion equations of the bushing on the vibrating plane were formed

$$m\ddot{x} + h_x \dot{x} + c_x x = mA\omega^2 \sin \omega t \cos \beta + F_{fr} \quad (1)$$

$$I\ddot{\varphi} + h_\varphi \dot{\varphi} + c_\varphi \varphi = T_{fr} \quad (2)$$

where

$$F_{fr} = -(\mu_1 + \mu_2) \left( \frac{1}{2} - \frac{1}{\pi} \right) (mg + c_y y_{st} - mA\omega^2 \sin \omega t \sin \beta) \times \text{sign} \dot{x}$$

$$T_{fr} = -(\mu_1 + \mu_2) \left( \frac{1}{3} - \frac{2}{3\pi} \right) (mg + c_y y_{st} - mA\omega^2 \sin \omega t \sin \beta) \times \left( \frac{R_2^3 - R_1^3}{R_2^3 - R_1^3} \right) \times \text{sign} \dot{\varphi}$$

where  $c_x = c_{x1} + c_{x2}$ ;  $c_y = c_{y1} + c_{y2}$ ;  $h_x = h_{x1} + h_{x2}$ .

The following non-dimensional parameters are used

$$\tau = \omega t; \quad \xi = \frac{x}{A}; \quad \gamma^2 = \frac{k^2}{\omega^2}; \quad \rho^2 = \frac{p^2}{\omega^2};$$

$$H_x = \frac{h_x}{m\omega}; \quad H_\varphi = \frac{h_\varphi}{mA^2\omega}; \quad \nu_\varphi = \frac{c_\varphi}{mA^2\omega^2};$$

$$\mu_\varphi = \frac{I}{mA^2}; \quad \nu = \frac{y_{st}}{A}; \quad \lambda = \frac{g}{A\omega^2}; \quad \delta = \frac{1}{A} \frac{R_2^3 - R_1^3}{R_2^3 - R_1^2}$$

where  $k^2 = c_x/m$ ;  $p^2 = c_y/m$ .

Then equations of bushing motion can be written in dimensionless form

$$\left. \begin{aligned} \ddot{\xi} + H_x \dot{\xi} + \gamma^2 \xi &= \sin \tau \cos \beta + f_{fr} \\ \mu_\varphi \ddot{\varphi} + H_\varphi \dot{\varphi} + \nu_\varphi \varphi &= \tau_{fr} \end{aligned} \right\} \quad (3)$$

where

$$f_{fr} = -(\mu_1 + \mu_2) \left( \frac{1}{2} - \frac{1}{\pi} \right) (\lambda + \rho^2 \nu - \sin \tau \sin \beta) \text{sign} \dot{\xi}$$

$$\tau_{fr} = -(\mu_1 + \mu_2) \left( \frac{1}{3} - \frac{2}{3\pi} \right) (\lambda + \rho^2 \nu - \sin \omega t \sin \beta) \delta \text{sign} \dot{\varphi}$$

The sign of friction force  $f_{fr}$  and friction moment  $\tau_{fr}$  depends on the body displacement and turn direction.

The sign “-” is used when  $Ox$  axis movement speed of the body is positive and turns counterclockwise and sign “+” represents motion of the body in opposite direction and turns clockwise.

Eq. (3) were solved numerical by using MatLab software package.

### 3. Simulation of the body displacement and turn controlled by dry friction

The vibrational displacement and turn of movably based body when dry friction coefficients are controlled by high frequency vibrations are examined (Figs. 2-9).

The most important for body motion character is parameter  $\gamma$ , which describes how the frequency of system's natural vibrations along  $\xi$  direction is related to excitement frequency. When the elastic resistance force is small, the body vibrates on the platform and moves forward (Fig. 2, a). The graphs show that when parameter  $\gamma$  increases, the body moves forward and later backwards (Fig. 3, a). The analysis of the motion characteristics indicates that if parameter  $\gamma$  increases, the body can move with jumping displacement and later vibrate close to the static equilibrium position (Fig. 4, a). Closely to dynamic equilibrium position, the body can move with jumping displacement and later vibrate with steady amplitude (Fig. 5, a). Vibrating near to the static equilibrium position, the amplitude of vibrations of the body can suddenly increase and after some time become steady (Fig. 6, a), can be vibrations with pulsating amplitude of the body (Fig. 7, a), slightly increase and become steady (Fig. 9, a). Fig. 8, a presents vibrations with nonstable amplitude.

With an increase in parameter  $\gamma$  both the character of the body movement and turn angle changes. It has been determined that the range of turn angle of the movably based part depends on stiffness coefficient  $\nu_\varphi$  of the turn in respect to connecting surfaces. If no angular resistance exists ( $\nu_\varphi = 0$ ), the body performs a forward slip vibrating and depend on value  $\gamma$  it can turn either counterclockwise (Fig. 2, b; 3, b; 6, b) or clockwise (Fig. 4, b; 5, b; 7, b; 9, b). If the stiffness coefficient of the turn is not equal to zero, the movably based body performs forward

movement and angular vibrations to the position of static equilibrium (Fig. 2, c). The body can turn both: counter-clockwise and clockwise (Fig. 8, b).

All displacement and turn regimes are formed when  $\gamma$  and  $\rho$  are different. Another parameters are the same:  $H_x = 0.01$ ;  $\beta = 0.3$ ;  $\lambda = 0.8$ ;  $\nu = 1.5$ ;  $\mu_\varphi = 200.0$ ;  $H_\varphi = 0.1$ ;  $\nu_\varphi = 0$ ;  $\delta = 100.0$ ;  $\mu_1 = 0.1$ ;  $\mu_2 = 0.4$ .

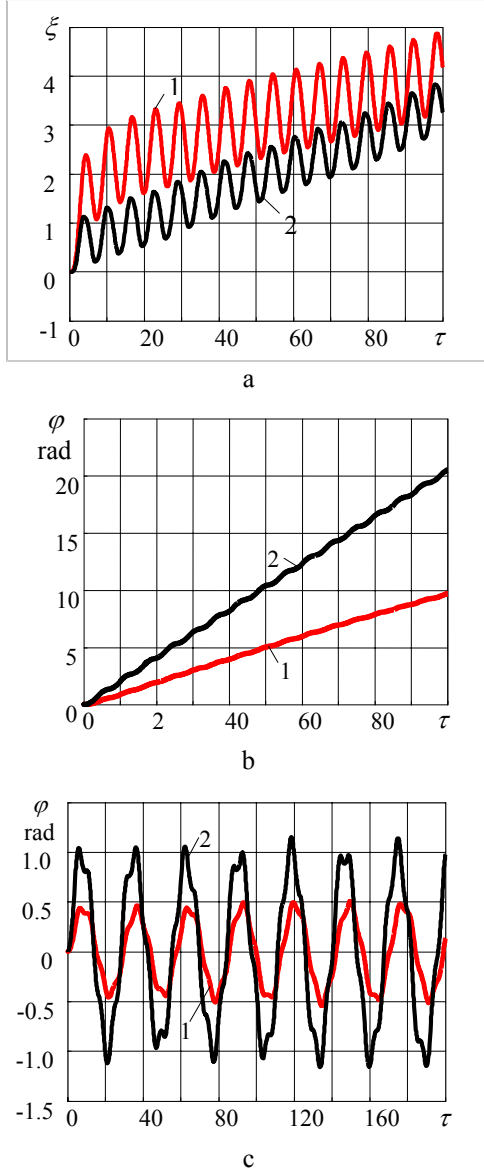


Fig. 2 Graphs of vibratory displacement (a), turn (b) and angular vibrations (c):  $\gamma = 0.025$ ,  $\rho = 1.8$ ; 1 -  $\mu_1 = 0.1$ ,  $\mu_2 = 0.2$ ; 2 -  $\mu_1 = 0.1$ ,  $\mu_2 = 0.4$ ; c -  $\nu_\varphi = 10$ ; 1 -  $\mu_1 = 0.1$ ,  $\mu_2 = 0.2$ ; 2 -  $\mu_1 = 0.1$ ,  $\mu_2 = 0.4$

Considering character of the motion trajectories it is possible to identify different regimes of the body motion, taking into account the sets of parameters  $\gamma$  and  $\nu$ , and the sets of parameters  $\gamma$  and  $\rho$  (Figs. 10 and 11).

According to the simulation results of the body displacement and its turn different regimes of the body movement in coordinates  $\gamma - \nu$  and  $\gamma - \rho$  have been determined. When the difference of dry friction coefficients is small ( $\mu_1 = 0.1$ ;  $\mu_2 = 0.2$ ) there are seven areas in  $\gamma - \nu$  coordinates (Fig. 10, a) and eight areas in  $\gamma - \rho$  coordinates (Fig. 11, a). If the difference of dry friction coefficients

is bigger ( $\mu_1 = 0.1$ ;  $\mu_2 = 0.4$ ) there are six areas in the  $\gamma - \nu$  and eight in  $\gamma - \rho$  coordinates [4].

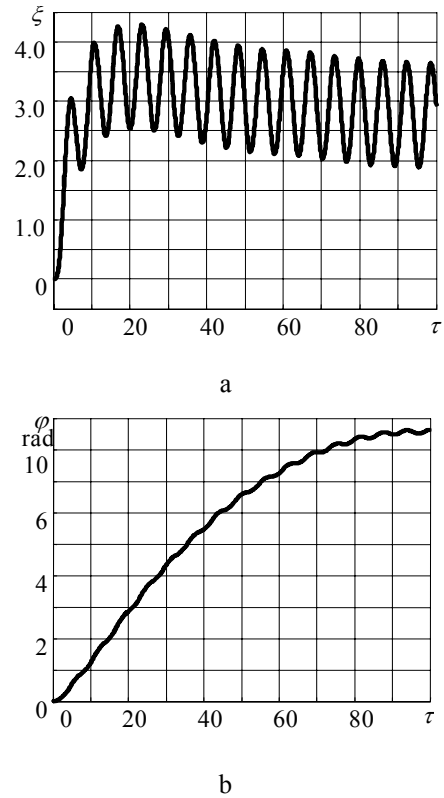


Fig. 3 Graphs of the body vibration on the platform and its movement forward and later backwards (a) and turn (b):  $\gamma = 0.060$ ,  $\rho = 1.1$

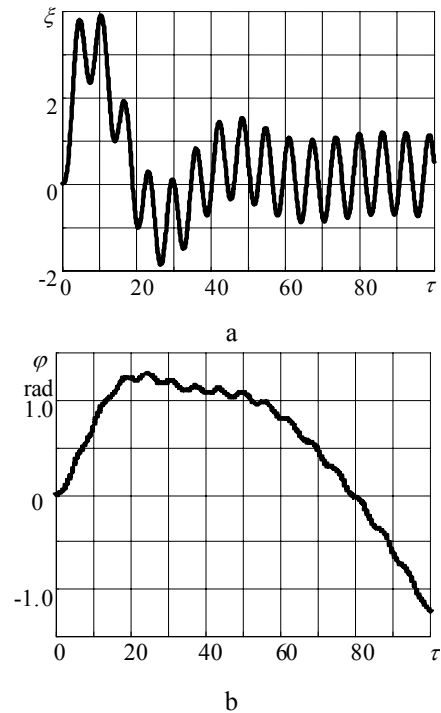


Fig. 4 Graphs of the body jumping movement and its vibration close to the position of static equilibrium (a) and turn (b):  $\gamma = 0.17$ ,  $\rho = 0.7$

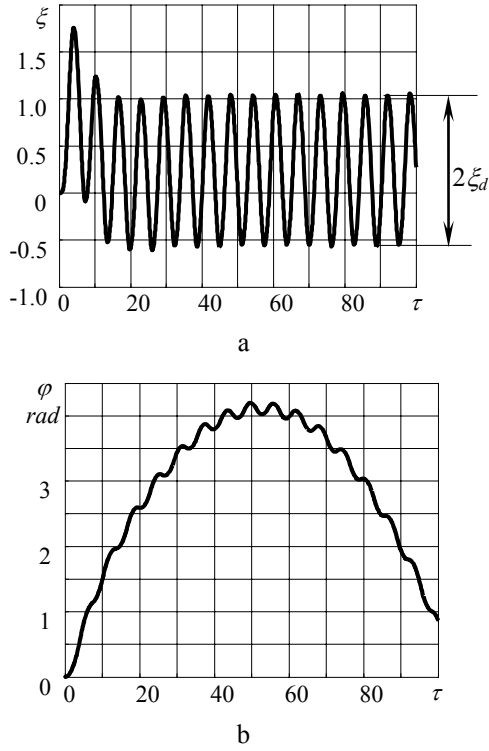


Fig. 5 Graphs of the body jumping movement and its vibration near to the position of dynamic equilibrium with steady amplitude (a) and turn angle (b):  $\gamma=0.25, \rho=1.5, \nu=1.5$

(Fig. 3, a). The first and second areas are too small and it's difficult to use these areas in practice. At particular parameters  $\gamma, \nu, \rho$  the body can perform jumping movement and afterwards vibrate close to the position of dynamic equilibrium (area 3) (Figs. 4, a; 5, a), vibrate close to the position of static equilibrium with steady amplitude (area 4) (Fig. 6, a).

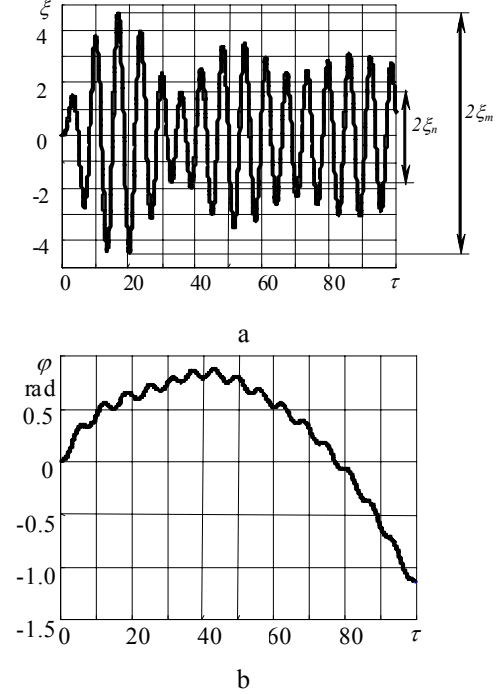


Fig. 7 Vibrations with pulsating amplitude of the body (a) and turn angle (b):  $\gamma=0.82, \rho=0.9$

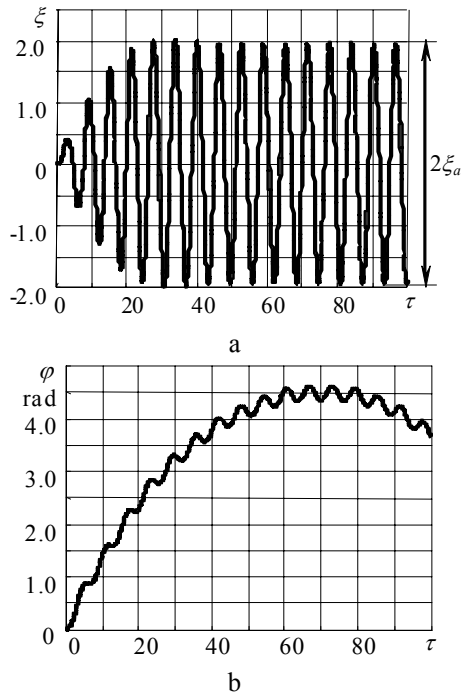


Fig. 6 The steady amplitude vibrations near to the position of static equilibrium (a) and turn angle (b):  $\gamma=1.16, \rho=1.9, \nu=1.5, \beta=0.3, \lambda=0.8, \mu_1=0.1, \mu_2=0.4$

If parameters  $\gamma, \nu$  and  $\rho$  belong to the first area (Figs. 10, 11), the body can move forward vibrating (Fig. 2, a) and also performing a counterclockwise turn (Fig. 2, b; 3, b; 6, b). In the second area, in coordinates  $\gamma-\nu$  and  $\gamma-\rho$  the regime of forward movement and later the backward movement backwards appears

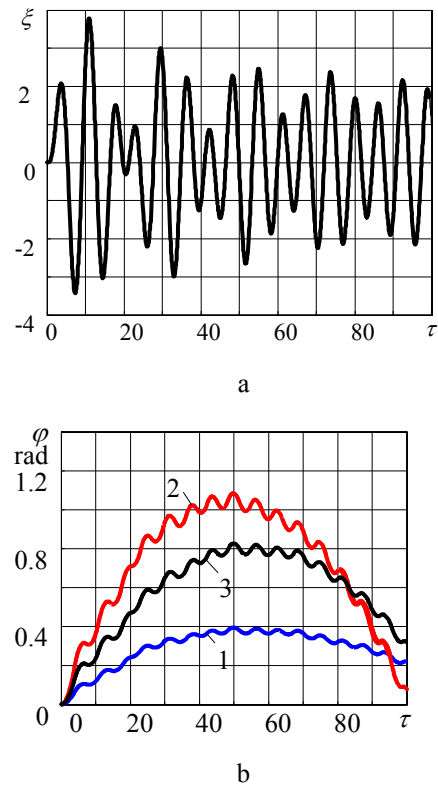


Fig. 8 Graphs of non stable vibrations (a) and turn angle (b):  $\gamma=0.67, \rho=0.9$ ; 1 -  $\mu_1=0.1, \mu_2=0.2$ ; 2 -  $\mu_1=0.1, \mu_2=0.3$ ; 3 -  $\mu_1=0.1, \mu_2=0.4$

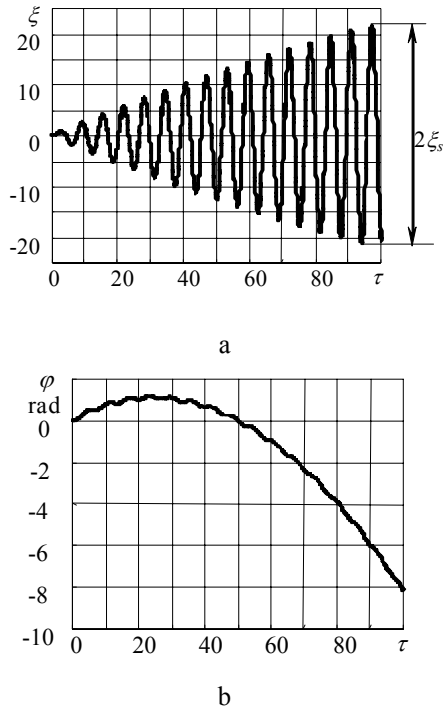


Fig. 9 Vibrations of the body close to the position of static equilibrium (a) and variation of the turn angle (b):  $\gamma=1.005, \rho=1.3, \nu=1.5$

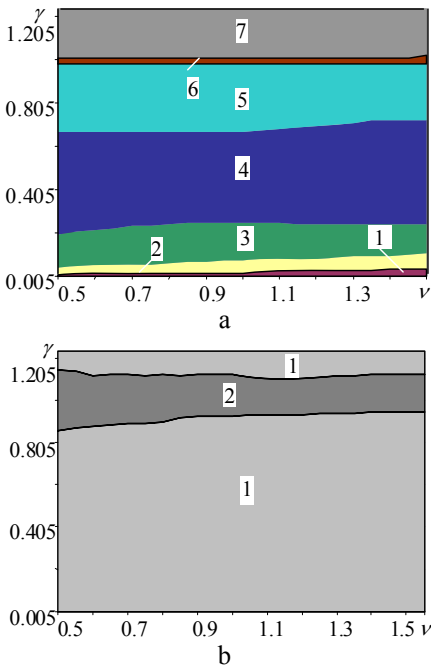


Fig. 10 Areas of  $\gamma$  and  $\nu$  parameters sets, which characterize regimes of the body motion when  $\mu_1=0.1, \mu_2=0.2$ : a – regimes of body movement; b – regimes of body turn: 1 - counterclockwise turn of the body; 2 - clockwise turn of the body

The fifth area in coordinates  $\gamma - \nu$  and the seventh area in coordinates  $\gamma - \rho$  present vibrations with pulsating amplitude (Fig. 7, a). The vibrations with increasing amplitude close to the position of static equilibrium (Fig. 9, a) are predetermined by parameter sets existing in the six  $\gamma - \nu$  and in the eighth  $\gamma - \rho$  areas. Vibration close to this position, the fifth area in coordinates

$\gamma - \rho$  represents how the amplitude of the body suddenly increases and after some time becomes steady [4]. The six area in coordinates  $\gamma - \rho$  is vibrations with nonstable amplitude (Fig. 8, a). In practice these areas are unusable for parts positioning. The Figs. 10, b and 11, b present the areas of the body turn.

The first area shows that body can turn counterclockwise and the second area shows clockwise turn of the body. It should be noted that the clockwise turn of the body (Figs. 4, b; 7, b; 9, b) is characteristic movement regimes at the third, sixth and seventh areas. The counterclockwise turn (Figs. 2, b; 3, b; 5, b; 6, b; 8, b) is appropriate for the first, second, fourth, fifth and eighth areas.

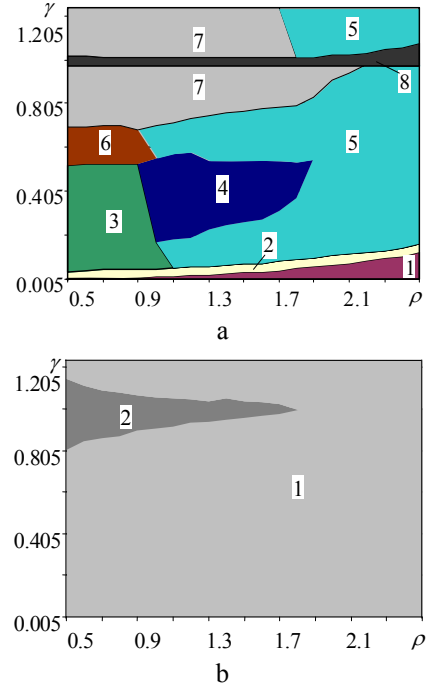


Fig. 11 Areas of parameters sets  $\gamma$  and  $\rho$ , characterizing the regimes of body movement when  $\mu_1=0.1, \mu_2=0.2$  respectively: a – regimes of body movement; b – regimes of body turn: 1 - counterclockwise turn of the body; 2 - clockwise turn of the body

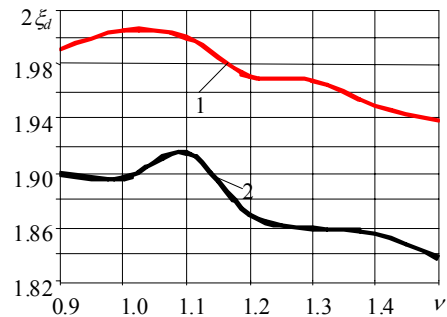


Fig. 12 Graphs of  $2\xi_d(\nu)$ :  $H_x=0.01, \beta=0.3, \lambda=0.8, \mu_\varphi=200, H_\varphi=0.1, \nu_\varphi=0, \delta=100, \gamma=0.24, \rho=1.2$ ; 1 -  $\mu_1=0.1, \mu_2=0.2$ ; 2 -  $\mu_1=0.1, \mu_2=0.4$

As the body performs a jumping displacement and afterwards vibrates near the position of dynamic equilibrium, double amplitude  $2\xi_d$  (Fig. 5, a) determines the

width of search area of matching surfaces. At increasing the parameter  $\nu$ , the double amplitude of vibrations  $2\xi_d$  decreases (Fig. 12). The dependencies are nonlinear. If parameter  $\gamma$  increases the double amplitude of vibrations  $2\xi_d$  also increases. When parameter  $\rho$  increases, the double amplitude of vibrations  $2\xi_d$  decreases [4].

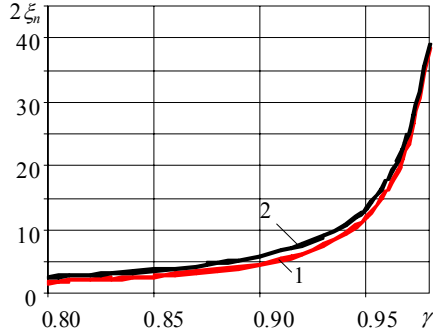


Fig. 13 Graphs of  $2\xi_n(\gamma)$ :  $H_x=0.01$ ,  $\beta=0.3$ ,  $\lambda=0.8$ ,  $\rho=0.8$ ,  $\mu_\varphi=200$ ,  $H_\varphi=0.1$ ,  $\nu_\varphi=0$ ,  $\delta=100$ ,  $\nu=1.1$ ;  $1 - \mu_1=0.1$ ,  $\mu_2=0.2$ ;  $2 - \mu_1=0.1$ ,  $\mu_2=0.4$

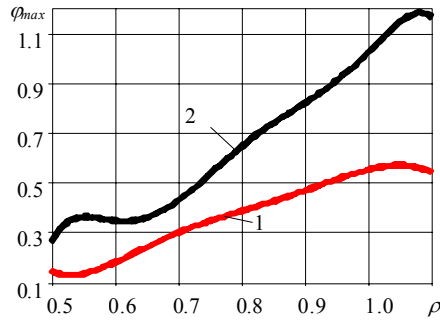


Fig. 14 Graphs of  $\varphi_{max}(\rho)$ :  $H_x=0.01$ ,  $\beta=0.3$ ,  $\lambda=0.8$ ,  $\gamma=0.80$ ,  $\mu_\varphi=200$ ,  $H_\varphi=0.1$ ,  $\nu_\varphi=0$ ,  $\delta=100$ ,  $\nu=1.1$ ;  $1 - \mu_1=0.1$ ,  $\mu_2=0.2$ ;  $2 - \mu_1=0.1$ ,  $\mu_2=0.4$

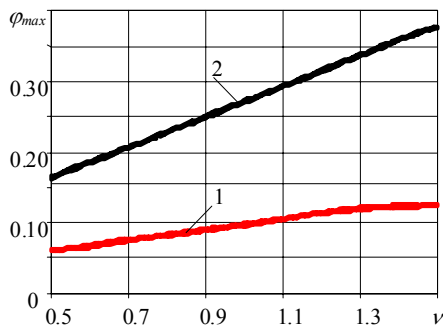


Fig. 15 Graphs of  $\varphi_{max}(\nu)$ :  $H_x=0.01$ ,  $\beta=0.3$ ,  $\lambda=0.8$ ,  $\rho=0.8$ ,  $\mu_\varphi=200$ ,  $H_\varphi=0.1$ ,  $\nu_\varphi=0$ ,  $\delta=100$ ,  $\gamma=0.99$ ;  $1 - \mu_1=0.1$ ,  $\mu_2=0.2$ ;  $2 - \mu_1=0.1$ ,  $\mu_2=0.4$

Under the regime of pulsating amplitude vibrations, when the body vibrates close to the position of static equilibrium, the amplitude may vary from  $2\xi_m$  to  $2\xi_n$  (Fig. 7, a). Value  $2\xi_m$  characterizes the maximum double pulsating amplitude and  $2\xi_n$  - minimum double pulsating amplitude. The values of these amplitudes greatly depend on parameters  $\gamma$ ,  $\rho$ . Maximum and minimum of the double amplitude depend on parameter  $\gamma$  (Fig. 13).

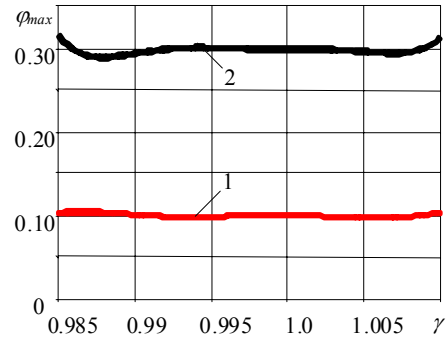


Fig. 16 Graphs of  $\varphi_{max}(\gamma)$ :  $H_x=0.01$ ,  $\beta=0.3$ ,  $\lambda=0.8$ ,  $\rho=0.8$ ,  $\mu_\varphi=200$ ,  $H_\varphi=0.1$ ,  $\nu_\varphi=0$ ,  $\delta=100$ ,  $\nu=1.1$ ;  $1 - \mu_1=0.1$ ,  $\mu_2=0.2$ ;  $2 - \mu_1=0.1$ ,  $\mu_2=0.4$

It has been determined by the analysis that when vibrations of the body are of the pulsating amplitude (Fig. 7, a), the maximum of turn angle  $\varphi_{max}$  depends on parameters  $\gamma$ ,  $\nu$ ,  $\rho$ . When the difference of the dry friction coefficients is bigger, the body can move to the longer distance and can turn to the greater angle. If parameters  $\rho$  (Fig. 14) and  $\nu$  (Fig. 15) increase, the  $\varphi_{max}$  also increases. The value of maximal turn angle  $\varphi_{max}$  practically not depends on the variation of parameter  $\gamma$  (Fig. 16).

#### 4. Schemes of vibratory assembly mechanisms

Based on results of the performed investigation, schemes of vibratory assembly mechanisms for automated assembly with noncircular cross-section were designed. Mutual orientation of the parts, applying vibratory alignment to one of the parts, ensures reliable positioning of both parts and their joining. Applied method of vibratory assembly under dry friction control allows little precision location of the parts in assembly position. For non-cylindrical form parts joining not only the displacement of the one part with respect of the other is necessary, but also particular turn of the part must be done.

Fig. 17 presents a scheme of the designed vibratory mechanism for noncylindrical shaped parts assembly. Bushing 11 is based at the center of the platform which consists of parts 6 and 17, having different coefficients of dry friction. The other part – shaft 12, is attached to the gripper 13 of the holder 16. When both the shaft 12 and the bushing 11 are in assembly position, their connective surfaces commonly are misaligned. The initial preload emerges as the gripper moves the shaft close to the bushing and by particular force presses the shaft 12 to the end of the bushing 11. By means of the rubber pad 19 the platform is divided into two parts and can freely move in the plane, perpendicular to the axes of the connective surfaces. Two piezoelectric vibrators 18 are attached to the different parts of the platform and excite the elastic vibrations. Due to two part division of the platform, under the control of dry friction the bushing is able not only to displace, but also is able to turn counterclockwise or clockwise in respect to the shaft. The alignment force displaces the platform with the bushing 11 and provides matching of the connective surfaces.





When the initial pressing force  $\nu$  of the body to the plane increases the double amplitude  $2\xi_d$  of vibration decreases. The higher is the difference in friction coefficients, the bigger is the angle of body turn.

3. For compensation of angular errors of mutual positioning of the parts the best is to apply such displacement regimes when the body vibrates close to the position of static equilibrium. Available combination of the values of  $\gamma$ ,  $\nu$  and  $\rho$  parameters exists, when the body can turn counterclockwise or clockwise.

4. Based on performed mutual positioning of the parts analysis the schemes of vibratory assembly devices, under control of the dry friction were designed. Those may be used for joining of the noncylindrical parts. Due to directional vibratory displacement and turn of the one part from the mating pair, there is no need for high accuracy of the parts placement in assembly position.

## References

1. **Sokolova, T., Bakšys, B.** Matching of connective surfaces controlling dry friction force.-Vibroengineering 2004: proceedings of 5th Int. Conference, October 14-15, 2004, Kaunas, Lithuania, ISSN 1392-8716, 2004, p.106-110.
2. **Setchi, R., Bratanov, D.** Three-dimensional simulation of accommodation.-Assembly Automation. -MCB University Press, 1998, v.18, No. 4, p.291-301.
3. **Edmondson, N.F., Redford, A.H.** A compliance device for flexible close tolerance. Industrial Robot. -An International Journal, 2001, v.28, No.1, p.54-62.
4. **Bakšys, B., Sokolova, T.** Vibratory displacement and turn of the body controlled by dry friction force.-Mechanika.-Kaunas: Technologija, 2004, Nr.1(45), p.44-50.
5. **Do, N. B., Ferri, A. A., Bauchau, O. A.** Efficient Simulation of a dynamic system with lugre friction. -Proc. ITDEC'05, ASME International Design Engineering Technical Conferences and Computers and Information in Engineering Conference, 2005, p.1-10.
6. **Fedaravičius, A., Tarasevičius, K., Bačkauskas, V.** Investigation of vibrotransportation on circularly moving platform with dry friction control. -Mechanika. -Kaunas: Technologija, 1998, Nr.3(14), p.40-46 (in Lithuanian).
7. **Graževičiūtė, J., Skiedraitė, I., Jūrėnas, V., Bubulis, A., Ostaševičius, V.** Applications of high frequency vibrations for surface milling. -Mechanika. -Kaunas: Technologija, 2008, Nr.1(69), p.46-49.

B. Bakšys, T. Sokolova

## NECILINDRINIŲ AUTOMATIŠKAI RENKAMŲ DETALIŲ TARPUSAVIO POZICIONAVIMAS

### Резюме

Straipsnyje nagrinėjamas necilindrinių automatiškai renkamų detalių pozicionavimas, valdant sausąją trintį. Sudarytas paslankiai bazuojamo kūno vibracinio poslinkio ir posūkio dinaminis modelis. Naudojant programų paketą MatLab sudarytos programos poslinkio ir posūkio reži-

mams apskaičiuoti. Pateiktos įvairios judėjimo režimų priklausomybės nuo sistemos ir žadinimo parametrų, atsižvelgiant į sausosios trinties koeficiento kitimo diapazoną. Svarbiausių parametrų plokštumoje sudarytos kūno judėjimo režimų, esant valdomajam sausosios trinties koeficientui egzistavimo sritys.

B. Bakšys, T. Sokolova

## MUTUAL POSITIONING OF AUTOMATICALLY ASSEMBLED NONCYLINDRICAL PARTS

### Summary

The paper examines the mutual positioning of noncylindrical parts by controlling dry friction applied for automated assembly. Dynamic model of vibratory displacement and turn is made. Using MATLAB software package for calculation of motion and turn regimes are developed. Graphical dependencies for amplitudes of body displacement both on the system and excitement parameters, taking into account dry friction coefficient in respect to excitation force period range, are given. The existing areas of the body displacement regimes at basic parameters plane when controlling dry friction were determined.

Б. Бакшис, Т. Соколова

## ВЗАИМНОЕ ПОЗИЦИОНИРОВАНИЕ ДЕТАЛЕЙ НЕЦИЛИНДРИЧЕСКОЙ ФОРМЫ ПРИ АВТОМАТИЧЕСКОЙ СБОРКЕ

### Резюме

В статье рассматривается взаимное позиционирование деталей нецилиндрической формы при управляемом сухом трении применительно к автоматической сборке. Составлена динамическая модель вибрационного перемещения и поворота подвижно базированного тела. Используя программный пакет MatLab составлены программы для расчета режимов движения и поворота тела. Представлены графические зависимости перемещения тела от параметров системы и возбуждения, учитывая изменения диапазона коэффициента сухого трения. В плоскостях главных параметров динамической системы и возбуждения составлены области существования для режимов движения тела при управляемом сухом трении.

Received December 02, 2008

Accepted March 03, 2009